

*Work supported in part by the Defense Research Board of Canada.

¹I. L. Ivanov and S. M. Ryvkin, *Zh. Tekhn. Fiz.* **28**, 774 (1958) [*Soviet Phys. Tech. Phys.* **3**, 722 (1958)].

²R. D. Larrabee and M. C. Steele, *J. Appl. Phys.* **31**, 1519 (1960).

³F. Okamoto, T. Koike, and S. Tosima, *J. Phys. Soc. Japan* **17**, 804 (1962).

⁴T. Misawa, *J. Appl. Phys. (Japan)* **1**, 130 (1962).

⁵B. B. Kadomtsev and A. V. Nedospasov, *J. Nucl. Energy* **1**, 230 (1960).

⁶M. Glicksman, *Phys. Rev.* **124**, 1655 (1961).

⁷Olvin Holter, *Phys. Rev.* **129**, 2548 (1963).

⁸C. E. Hurwitz and A. L. McWhorter, *Phys. Rev.* **134**, A1033 (1964).

⁹E. M. Conwell, in *Solid State Physics, Supplement* (Academic, New York, 1967), Vol. 9.

¹⁰R. A. Smith, *Semiconductors* (Cambridge U. P., New York, 1959), p. 160.

¹¹K. Ando and M. Glicksman, *Phys. Rev.* **154**, 316 (1967).

¹²W. S. Chen and B. Ancker-Johnson, *Appl. Phys. Letters* **15**, 59 (1969).

PHYSICAL REVIEW B

VOLUME 2, NUMBER 2

15 JULY 1970

Exact Solution of a Boltzmann-Equation Model for Oscillatory Photoconductivity*

N. O. Folland

Kansas State University, Manhattan, Kansas 66502

(Received 26 January 1970)

The photoconductive response of some semiconductors to monoenergetic excitation shows structure which is associated with the emission of optical phonons. A model for oscillatory photoconductivity based on the Boltzmann equation has been suggested and partly investigated by Stocker and Kaplan (SK). An exact solution of the SK Boltzmann equation is presented in this paper. A model valid for small electric fields is derived from the exact solution which retains the main features of the SK model in a form particularly amenable to calculation. The properties of the small-field model are illustrated by two series of calculations. In the first series of calculations, the composition of a dip in the photoresponse caused by the proximity of an optical phonon emission threshold to the electron injection energy is analyzed. The shape and "intensity" of a dip depend on the relative values of the recombination lifetime, the strength of acoustical and optical phonon scattering, and the electric field. A second series of calculations was designed to show how the periodic repetition of dips in the photoresponse as a function of electron injection energy can be inhibited or destroyed by competition from other optical phonons.

I. INTRODUCTION

The photoconductive response of certain semiconductors exhibits periodic dips as a function of the monoenergetic exciting radiation. These "oscillations" were first observed in the extrinsic photoconductivity of the InSb:Cu system¹ and have since been seen in many systems.² More recent observations of the extrinsic photoconductivity of Si have revealed dips which are repeated no more than once, if at all.³ In all cases, the dips are thought to arise from the onset of optical phonon emission.

The phenomenon has been treated theoretically in terms of a model based on the Boltzmann equation.⁴ The main innovation of the Stocker-Kaplan (SK) model as compared with similar models for electron transport⁵ is the explicit inclusion of an electron generation term. It is this property of the SK model which suggested a scheme leading to an exact solution.

The theoretical development of the SK model as described in the original paper⁴ is inadequate in several respects. First, the calculations are based on an expansion in spherical harmonics of the Boltzmann distribution function in which only the first two terms are retained. This truncation approximation is arbitrary and the resulting equations are complicated. A solution was found only for a limited region and special circumstances. Second, the calculations do not consider more than one type of optical phonon process. The experimental results for Si, which has three distinct optical phonon processes operative,⁶ suggest that there is a competition between the various optical phonon emission processes that tends to prevent the periodic repetition of the dips. Even accepting the truncation approximation, it is not clear that the original treatment can be extended to include more than one type of phonon process.

It is the purpose of this paper to present an exact

solution of the SK model appropriate to steady-state conditions. The original description of the SK model is generalized (trivially) to include multiphonon emission and all orders in the expansion in spherical harmonics. A model for photoconductivity is derived from the exact distribution function which includes in a physically realizable context the principal content of the SK model in a form suitable for calculation.

The SK model is reviewed in Sec. II. The exact steady-state solution is derived in Sec. III. A model for photoconductivity valid for small, but finite, electric fields is derived and some of its properties exhibited in Sec. IV. In Sec. V, the results of the paper are summarized and discussed.

II. STOCKER-KAPLAN MODEL

The SK model is based on the Boltzmann equation. The model describes an electronic system in which phonon interactions are included to the extent that they lead to electronic transitions. Modifications of the electronic excitation spectrum due to electron-phonon coupling are not considered. Electron densities are sufficiently low that electron-electron interaction and effects of the Pauli-exclusion principle can be ignored. A detailed discussion of the limitations on the physical systems for which the SK model is applicable and the assumptions regarding the type and form of the scattering processes is given in Ref. 4. We review here only those features of the model which are essential for the subsequent development.

The electronic system consists of electrons which have been excited into a parabolic band. With respect to the band minimum, electronic excitation energies are given by

$$E(\vec{k}) = \sum (\hbar k_i)^2 / 2m_i, \quad (1)$$

where the electron momentum \vec{k} is also referred to the band minimum. Let $N(\vec{k}, t)$ be the number of electrons in electronic state \vec{k} and unspecified spin. Then, the Boltzmann equation is

$$\frac{\partial N}{\partial t}(\vec{k}, t) = \dot{N}(\vec{k}, t)_{\text{inj}} - \dot{N}(\vec{k}, t)_{\text{rec}} - (e\vec{E}/\hbar) \cdot \vec{\nabla}_{\vec{k}} N(\vec{k}, t) + \sum_p \sum_{\vec{k}'} [N(\vec{k}', t) \Gamma_{\vec{k}, \vec{k}'}(p) - N(\vec{k}, t) \Gamma_{\vec{k}', \vec{k}}(p)], \quad (2)$$

where in addition to the usual electric field and master-equation terms (ignoring Pauli-exclusion-principle effects), injection and recombination terms have been included explicitly.

The form of the transition rates is determined by the Golden Rule where for the phonon scattering process p ,

$$\Gamma_{\vec{k}, \vec{k}'}(p) = (2\pi/\hbar) |H_{\vec{k}, \vec{k}'}(p)|^2$$

$$\times \delta[E(\vec{k}) - E(\vec{k}') \pm \xi_p(\vec{k} - \vec{k}')] \quad (3)$$

It is convenient to transform the sums over electronic states to integrals and scale k space, $k_i'' = \hbar k_i / \sqrt{2m_i}$. Thus, if we let

$$D = [m_1 m_2 m_3 / (m_0 \text{Ry})^3]^{1/2} 2V / (2\pi a_0)^3,$$

with $a_0 = 0.5292 \text{ \AA}$, $\text{Ry} = 13.605 \text{ eV}$, and m_0 the electron rest mass, then for an arbitrary function $B = B(\vec{k}, \vec{k}')$,

$$\sum_{\vec{k}} \Gamma_{\vec{k}, \vec{k}'}(p) B = \int d^3 k'' (g_p / 2\pi) \delta[k''^2 - E(\vec{k}') \pm \xi_p] B, \quad (4)$$

where the coupling parameter g_p is given by

$$g_p = D |H_{\vec{k}, \vec{k}'}(p) 2\pi|^2 / \hbar \quad (5)$$

In the SK model, the lifetimes are taken to be constant or dependent upon the energy of the initial state. Similarly, the momentum dependence of the energy lost or gained ξ_p in inelastic scattering processes (optical phonons) is neglected.

Two cases are treated in our application of Eq. (4). If B is independent of k'' and g_p is constant, we obtain the lifetime (written for phonon emission)

$$1/\tau_p(k') = g_p (k'^2 - \xi_p)^{1/2} \theta(k'^2 - \xi_p), \quad (6)$$

where $E(k') = k'^2$ is the energy of the initial electronic state and $\theta(x) = 0(1)$ if $x < (>) 0$. The case, where B depends on \vec{k}'' can also be expressed in terms of the lifetime. Let $B_0(k)$ be the spherical average of $B(\vec{k})$. Then,

$$\int d^3 k'' (g_p / 2\pi) \delta(k''^2 - k'^2 - \xi_p) B(\vec{k}'') = B_0(k'^2 + \xi_p)^{1/2} \tau_p(k'^2 + 2\xi_p)^{1/2}. \quad (7)$$

Electrons may be scattered by optical phonons, acoustical phonons, and impurities. Temperatures are considered to be sufficiently low that only optical phonon emission is probable. Scattering by impurities and acoustical phonons is taken to be elastic ($\xi_a = \xi_i = 0$).

A key feature of the SK model is that the electrons are injected monoenergetically and uniformly into the conduction band. Thus, if \dot{N}_0 is the rate at which electrons are injected into states of energy E_0 , then the injection term may be written

$$\dot{N}(\vec{k}, t)_{\text{inj}} = (\dot{N}_0 / 2\pi \sqrt{E_0}) \delta[E(\vec{k}) - E_0] / D. \quad (8)$$

The recombination processes are represented by a recombination lifetime τ_r such that

$$\dot{N}(\vec{k}, t)_{\text{rec}} = N(\vec{k}, t) / \tau_r. \quad (9)$$

It is convenient to define a new electron distribution function $f(\vec{k}', t) = D N(\vec{k}, t)$ such that

$$\sum_{\vec{k}} N(\vec{k}, t) = \int d^3 k' f(\vec{k}', t).$$

Incorporating the definitions and specializations described above into the original Boltzmann equation (2), we obtain the SK model in the form

$$\frac{\partial}{\partial t} f(\vec{k}, t) = \frac{\dot{N}_0 \delta(k^2 - k_0^2)}{(2\pi k_0)} - \frac{f(\vec{k}, t)}{\tau_r} - \vec{F} \cdot \vec{\nabla}_{\vec{k}} f(\vec{k}, t) + \sum_p \left(\frac{f_0(k^2 + \xi_p)^{1/2}}{\tau_p(k^2 + 2\xi_p)^{1/2}} - \frac{f(\vec{k}, t)}{\tau_p(k)} \right). \quad (10)$$

In Eq. (10), we recognize that $E(k) = k^2$, $E_0 = k_0^2$ and that $F_i = eE_i / \sqrt{2m_i}$ is the scaled form of the electric field.

It should be emphasized that Eq. (10) is not identical to the original SK Boltzmann equation as given in Ref. 4. In obtaining Eq. (10), the coupling parameter g_p of Eq. (5) was taken to be a constant as is more appropriate for nonpolar crystals. If instead we take $g_p = 2D' / (\vec{k} - \vec{k}')^2$ with

$$D' = e^2 \xi_p (1/\epsilon_\infty - 1/\epsilon_0) (2m^*/\hbar^4)^{1/2},$$

then the lifetime corresponding to our Eq. (6) and Eq. (25) of Ref. 4 is

$$1/\tau_p(k) = (D'/k) \cosh^{-1}(k/\sqrt{\epsilon_p}).$$

Thus, the last term in Eq. (10) has the same form for both cases. An important difference arises in the term which represents inelastic scattering into a state \vec{k} . In evaluating Eq. (7) with the k -dependent coupling parameter, all orders in an angular expansion occur. The rate at which electrons are scattered into a state \vec{k} is found to be

$$R(\vec{k}) = D' \sum_m (k^2 + \xi_p)^{1/2} (2m+1) f_m(k^2 + \xi_p)^{1/2} \times C_m[k, (k^2 + \epsilon_p)^{1/2}],$$

where in terms of the Legendre polynomials P_m ,

$$f_m(k') = \frac{1}{4\pi} \int d\Omega_{\vec{k}'} f(\vec{k}') P_m(\hat{k} \cdot \hat{k}')$$

$$\text{and } C_m(k, k') = \int_{-1}^1 dx P_m(x) / (k^2 + k'^2 - 2kk'x).$$

The first term in the series is the term which appears in the SK Boltzmann equation.⁴ This term may be written in terms of the lifetime as

$$R_0(k) = f_0[(k^2 + \epsilon_p)^{1/2}] [(k^2 + \xi_p)^{1/2}/k] \tau_p^{-1} (k^2 + \xi_p)^{1/2}.$$

The development which follows is based on Eq. (10) above. However, it is not difficult to modify the theory to include this polar k dependence of the coupling parameters. The modification is trivial if one chooses to include only the first term in the series. In fact the steady-state solution based on any truncated expansion is still exact to the order of truncation.

III. EXACT SOLUTIONS FOR STEADY STATE

In terms of Eq. (10), the steady-state condition

is that $(\partial/\partial t)f(\vec{k}, t) = 0$. We have not considered transient or time-dependent effects. However, the method of solution which is applied to the steady-state problem in the presence of finite electric fields might be generalized to treat some time-dependent effects.

A. No-Field Case

Some of the important features of the SK model are illustrated by the exact solution of the steady-state problem in the absence of an electric field. Without the electric field, there is no preferred direction in momentum space and the distribution function must be spherically symmetric. Hence, the elastic scattering processes ($\xi_p = 0$) are automatically balanced and they drop out of the Boltzmann equation. Furthermore, from the description of the model in Sec. II, we expect the electrons to form a ladder in energy whose upper rung is determined by the injection energy and lower rungs determined by the competition between the optical phonon and the recombination processes. Of course, the base of the ladder corresponds to the conduction-band minimum.

The solution may be expressed quantitatively as depicted above,

$$f_0(k) = \sum f_0^j(k), \quad (11)$$

where each term f_0^j , $j = 1, \dots$ corresponds to a set of "rungs" generated by optical phonons. Let

$$1/\tau(k) = 1/\tau_r + \sum_{p \neq c} 1/\tau_p(k)$$

define a total lifetime for electrons with energy k^2 , but excluding conservative processes. The first rung of the ladder is

$$f_0^1(k) = \dot{N}_0 \tau(k) \delta(k^2 - k_0^2) / (2\pi k_0). \quad (12)$$

And succeeding sets of rungs are given by the recursion relation

$$f_0^{j+1}(k) = \sum_{p \neq c} f_0^j[(k^2 + \xi_p)^{1/2}] \tau(k) / \tau_p[(k^2 + 2\xi_p)^{1/2}]. \quad (13)$$

It is easy to verify that Eqs. (11)–(13) are a solution of the no-field case of Boltzmann Eq. (10).

B. Finite Electric Fields

The effect of the electric field will be to shift the spherical surfaces in momentum space which formed the rungs of the ladders in energy in the case of zero field. It is evident that there will be a region of field strengths centered about zero which are sufficiently small that the main features of the ladder picture are retained. Thus, we are motivated to cast our solution for finite fields after the ladder picture.

In essence, the approach amounts to following an

electron from its injection into the conduction band through its many paths toward recombination. For this purpose, it is useful to distinguish the conservative (energy) decay modes from the inelastic modes. Let $1/\tau_c = 1/\tau_i + 1/\tau_a$ be the decay rate for the conservative processes, impurity, and acoustic phonon scattering. Then, $1/\tau_T = 1/\tau_c + 1/\tau$ is the decay rate for all processes.

If the injection rate is \dot{N}_0 , then between times $t = 0$ and $t = dt$, $dN_0 = \dot{N}_0 dt$ electrons will have been injected. Thus, the number of electrons from the original dN_0 which have not been scattered in any way after time t will be $dN_0 \exp[-\int_0^t dt' / \tau_T(t')]$. However, it does not suffice merely to count the electrons, their momentum must also be monitored. If an electron initially has momentum \vec{k}_1 and it is not scattered, then only the electric field influences it, $\vec{k}_2 = \vec{k}_1 + \vec{F}t$. Hence, if electrons are being continuously injected at unit rate, the distribution in momentum space $G_u(k_1, k_2)$ of particles which have not been scattered at all is independent of time:

$$G_u(k_1, \vec{k}_2) = \frac{1}{4\pi} \int d\Omega(\hat{k}_1) \int_0^\infty dt \exp[-\int_0^t dt' / \tau_T] \times (|\vec{k}_1 + \vec{F}t'|) \delta(\vec{k}_2 - \vec{k}_1 - \vec{F}t'). \quad (14)$$

The spherical average in Eq. (14) on \vec{k}_1 makes the injection uniform in momentum space. It is easy to show that $G_u(\vec{k}_1, \vec{k}_2)$ satisfies the differential equation

$$[\vec{F} \cdot \vec{\nabla}_2 + 1/\tau_T(k_2)] G_u(k_1, \vec{k}_2) = \delta(k_1^2 - k_2^2) / (2\pi k_1). \quad (15)$$

In the absence of an electric field, conservative processes were automatically balanced in the Boltzmann equation. This suggests that we treat these separately. Since G_u is defined for unit injection rate and the rate at which electrons are scattered by conservative processes from momentum state \vec{k}_3 is $G_u(k_1, \vec{k}_3) / \tau_c(k_3)$, it follows that the distribution function G_c for electrons which are scattered conservatively, if at all, satisfies the recursion relation

$$G_c(k_1, \vec{k}_2) = G_u(k_1, \vec{k}_2) + \int d^3k_3 [G_u(k_1, \vec{k}_3) / \tau_c(k_3)] G_c(k_3, \vec{k}_2). \quad (16)$$

In the case of zero field, we see that $\dot{N}_0 G_c(k_0, \vec{k}) = f_0^1(k)$, where f_0^1 is given by Eq. (12). The distribution function $G_c(k_0, \vec{k})$ satisfies

$$[\vec{F} \cdot \vec{\nabla}_2 + 1/\tau_T(k_2)] G_c(k_1, \vec{k}_2) = \delta(k_1^2 - k_2^2) / (2\pi k_1) + G_0^0(k_1, k_2) / \tau_c(k_2). \quad (17)$$

Hence, $\dot{N}_0 G_c$ would be an exact solution of the Boltzmann equation if there were no optical phonons.

The inelastic scattering by optical phonons is included in the distribution function $G(k_1, \vec{k}_2)$ by the same reasoning that leads to Eq. (16),

$$G(k_1, \vec{k}_2) = G_c(k_1, \vec{k}_2) + \sum_{p \neq c} \int d^3k_3 [G_c(k_1, \vec{k}_3) / \tau_p(k_3)] \times G[(k_3^2 - \xi_p)^{1/2}, \vec{k}_2]. \quad (18)$$

The distribution function $f(\vec{k}) = \dot{N}_0 G(k_0, \vec{k})$ is an exact solution of the steady-state case of the Boltzmann equation (10). Furthermore, the series development of Eq. (18) reduces exactly to Eqs. (11)–(13) when the field is zero.

As originally treated,⁴ the SK model approximated the Boltzmann equation by an expansion in Legendre polynomials truncated after two terms. A first step towards comparing the exact solution to the SK results is to expand G_u in Legendre polynomials:

$$G_u(k_0, \vec{k}) = \sum_m \frac{(2m+1)}{8\pi k_0 k F} P_m(\hat{k} \cdot \hat{F}) \int_{|k_0-k|}^{k_0+k} \frac{dt}{t} \times \exp\left(-\int_0^t \frac{dt'}{F \tau_T(|k_0 + F t'|)}\right) P_M\left(\frac{t^2 + k^2 - k_0^2}{2kt}\right), \quad (19)$$

where \hat{F} is the axis of cylindrical symmetry and $\vec{k}_0 \cdot \hat{F} = (k^2 - k_0^2 - t^2) / 2t$.

The expansion in Legendre polynomials Eq. (19) should be of general value because any average that one might wish to take with respect to the steady-state Boltzmann function should be decomposable into terms of the form

$$A_m(k_0) = \int d^3k G_u(k_0, k) R_m(k) P_m(\hat{k} \cdot \hat{F}), \quad (20)$$

where R_m is an arbitrary function. However, the singularity in Eq. (19) at $t = 0$ can be annoying in numerical applications. We describe below a transformation which serves to remove the singularity and simplify the form of the integrals.

In Fig. 1 is sketched the region of integration of the two variables k and t which remain in Eq. (20) upon completion of the angular integration. The vertical broken line shows the restriction on the range of the t integration for a typical value of k . Consider the transformation on k , $k^2 = k_0^2 + t(t - 2y)$, where $|y| \leq k_0$ as t ranges from zero to infinity. A y -integration path for a typical value of t is given by the horizontal broken line in Fig. 1, and Eq. (20) becomes

$$A_m(k_0) = \frac{1}{2k_0 F} \int_{-k_0}^{k_0} dy \int_0^\infty dt R_m(k)$$

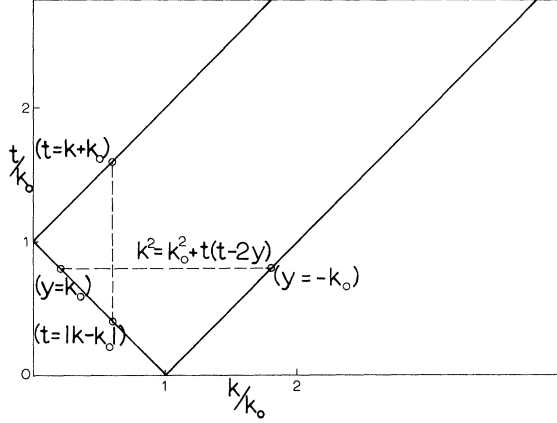


FIG. 1. Transformation of the two-dimensional integral on variables k and t in Eq. (20). In Eq. (20), k ranges from zero to infinity. For each value of k , t is restricted to $|k - k_0| \leq t \leq k + k_0$ as indicated for a typical case by the vertical broken line. In the transformed equation (21), t ranges from zero to infinity and the new variable y is bounded, $|y| \leq k_0$, as shown by the horizontal broken line. For fixed t , k and y are related by $k^2 = k_0^2 + t(t - 2y)$.

$$\times \exp\left(-\int_0^t \frac{dt'}{F\tau_T(|\vec{k}_0 + \hat{F}t'|)}\right) P_m\left(\frac{t-y}{k}\right), \quad (21)$$

where $k^2 = k_0^2 + t(t - 2y)$ and $\vec{k}_0 \cdot \hat{F} = -y$. This result finds immediate application in the calculation of the photoresponse current for the SK model.

C. Steady-State Photocurrent

In the SK model, monoenergetic carriers are being injected uniformly into the conduction band. It is the response of these carriers to an electric field which is measured experimentally. The photoresponse current in the SK model is defined by $J(E_0) = \sum N(\vec{k}) e \vec{v}(\vec{k})$, where $v_i(k) = \hbar k_i / m_i$ is the particle velocity and E_0 is the injection energy. Making the sum an integral and transforming to spherical bands the current

$$J_i(E_0) = e N_0 (2/m_i)^{1/2} K_i(k_0) / V \quad (22)$$

is conveniently expressed in terms of a reduced current

$$\vec{K}(k_0) = \int d^3k f(\vec{k}) \vec{k} / N_0 = \int d^3k G(k_0, \vec{k}) \vec{k}, \quad (23)$$

where $E_0 = k_0^2$ and G is defined by Eq. (18). Similarly, we may define unscattered and conservative reduced currents after the distribution functions defined in Eqs. (14) and (16)

$$K_m(k_0) = \int d^3k G_m(k_0, \vec{k}) \vec{k}, \quad (24)$$

with $m = u$ or c .

The only nonzero component of the unscattered

current is in the direction of the electric field \hat{F} and only the second term in the Legendre polynomial expansion contributes:

$$K_u(k_0) = \frac{1}{2k_0 F} \int_{-k_0}^{k_0} dy \int_0^\infty dt (t - y) \times \exp\left(-\int_0^t \frac{dt'}{F\tau_T(|\vec{k}_0 + \hat{F}t'|)}\right). \quad (25)$$

Hence, the conservative current is in the \hat{F} direction and it is determined by

$$K_c(k_0) = K_u(k_0) + \int d^3k' G_u(k_0, \vec{k}') K_c(k') / \tau_c(k'). \quad (26)$$

The total current is also in the \hat{F} direction and it is determined by

$$K(k_0) = K_c(k_0) + \sum_{p \neq c} \int d^3k' G_c(k_0, \vec{k}') \times K[(k'^2 - \xi_p)^{1/2}] / \tau_p(k'). \quad (27)$$

IV. SMALL-FIELD BEHAVIOR

Most physical effects of interest are realized at relatively small fields. For example, in the intrinsic photoconductivity of InSb² the oscillatory effect is clearly observed at electric field intensity 5 mV/cm and it has almost disappeared at 7 V/cm.

It is our intention here to illustrate by detailed calculation the properties of the SK model for small electric fields.

A. Small-Field Model

A qualitative criterion for the smallness of an electric field is that the ladder picture of Sec. IIIA be essentially preserved. As can be seen from Eq. (14), a quantitative estimate of field strength is

$$F\tau_T \approx (E \text{ cm/V}) (\tau_T / 10^{-12} \text{ sec}) (\text{meV})^{1/2} / 1000,$$

the momentum transferred (scaled units) by an electric field E to an electron during its lifetime τ_T . This suggests that a good approximation for the distribution of electrons which have been scattered conservatively, if at all, may be obtained by replacing G_u in the integral term of Eq. (16) by the corresponding expression for the zero-field case,

$$G_c(k_0, \vec{k}) = G_u(k_0, \vec{k}) \tau(k_0) / \tau_T(k_0). \quad (28)$$

The approximation leading to Eq. (28) is most likely to fail when the injection energy is near a phonon emission threshold. However, since the applications of interest are at low temperatures where acoustic phonon scattering is weak and impurity concentrations are low, corrections to the conservative distribution function Eq. (28) should be small.

Actually, the relevant lifetime for preserving the ladder picture is not the total lifetime τ_T , but only the nonconservative part τ . Thus, for the SK model the recombination lifetime τ_r places an upper bound $F\tau_r$ on the estimated widths.

Similarly, the contribution to the current from electrons injected into the conduction band at energy k_0^2 and which are scattered conservatively, if at all, is approximated by

$$K_c(k_0) = K_u(k_0) \tau(k_0) / \tau_T(k_0). \quad (29)$$

In treating Eq. (27), it is tempting to evaluate the integral by taking the distribution function G_c in the small-field limit as was done to obtain Eq. (29). In this approximation, the currents form a ladder with rungs specified by the recursion relation

$$K(k_0) = K_c(k_0) + \sum_{p \neq c} K[k_0^2 - \xi_p]^{1/2} \frac{\tau(k_0)}{\tau_T(k_0)} / \tau_p(k_0). \quad (30)$$

However, as mentioned above, when the injection energy is so near an optical phonon emission threshold that it is probable that the field can take it over the threshold, then it may not be a good approximation to replace the energy-dependent electron lifetime by its value at the point of injection.

Electrons may be injected into the conduction band near a phonon emission threshold either directly or by cascading down the ladder. A threshold term of the current ladder is best treated separately. This "threshold" current has the form

$$K_t(k_0) = \int d^3 k' G_c(k_0, \vec{k}') K_c[k'^2 - \xi_p]^{1/2} / \tau_p(k'), \quad (31)$$

where it is understood that $k_0^2 \sim \xi_p$. The current near the bottom of the conduction band is primarily limited by the recombination lifetime in the SK model. From Eqs. (25) and (29) it may be seen that for $k_0 \sim 0$,

$$K_c(k_0) = \tau_r \tau_T(k_0) F. \quad (32)$$

Thus, if Eq. (32) is used for the current in the integrand of Eq. (31), then the transformation of Eqs. (20) and (21) leads to an expression for the threshold current,

$$K_t(k_0) = \frac{1}{2k_0} \int_{-k_0}^{k_0} dy \int_0^\infty dt \exp\left(-\int_0^t \frac{dt'}{F\tau_T(|\vec{k}_0 + \hat{F}t'|)}\right) \times \frac{\tau(k_0)\tau_T[(k'^2 - \xi_p)^{1/2}]\tau_r}{\tau_T(k_0)\tau_p(k')}, \quad (33)$$

where $k'^2 = k_0^2 + t(t - 2y)$ and $\vec{k}_0 \cdot \hat{F} = -y$. Equation (33) has the same form as Eq. (25) and in this sense, at least, is suitable for numerical work.

The small-field model for oscillatory photoconductivity consists of a ladder of conservative currents, Eqs. (29) and (25). The rungs of the ladder recur according to Eq. (30) except for a rung or

part of a rung in which electrons are injected near a phonon emission threshold. Then, the last current in the ladder is given by Eq. (33).

The small-field model described above retains those parts of the SK model which lead to structure in the photoconductive response. The model neglects some effects on the electron distribution from acoustic phonon or impurity scattering. These can be minimized in an experiment. In this model, the current resulting from injection near an optical phonon emission threshold are treated exactly. However, field effects are neglected entirely in the cascade down to a phonon emission threshold. For many purposes, given realistic scattering rates, the small-field model will exhaust the possibilities of the SK model for describing oscillatory photoconductivity.

B. Calculations

The calculations are based on the small-field model as described above. Only phonon scattering and recombination processes are considered. The phonon scattering rates are taken in the form of Eq. (6) with a constant coupling parameters. Thus, the model will provide a fairly realistic description of phonon scattering in nonpolar semiconductors. The first optical phonon emission threshold serves as a reference point. Let the lowest-energy optical phonon have energy 16 meV and coupling constant $g_1 = 10^{12}(\text{meV})^{1/2}/\text{sec}$. The coupling parameters describing any other phonons which are introduced will be given relative to g_1 . For lack of anything better, the recombination lifetime is taken to be a constant.

The exponent in Eqs. (25) and (33) for the above scattering rates is proportional to

$$\int_0^t \frac{dt'}{\tau_T(|\vec{k}_0 + \hat{F}t'|)} = \frac{t}{\tau_r} + \sum_p \frac{g_p}{2} \left((t-y)r_{1p} + y r_{0p} + \frac{1}{2}(k_0^2 - y^2 - \xi_p) \ln \left| \frac{(t-y+r_{1p})(y+r_{0p})}{[(t-y-r_{1p})(y-r_{0p})]} \right| \right), \quad (34)$$

where $r_{1p} = (k_i^2 - \xi_p)^{1/2} \theta(k_i^2 - \xi_p)$ with $k_{i=0} = k_0$ and $k_i^2 = k_0^2 + t(t - 2y)$. Using Eq. (34) for the exponent, Eqs. (25) and (33) are completely straightforward to integrate numerically. Note that the coefficient of the logarithm term of Eq. (34) approaches zero in the same way that any factor in the argument of the logarithm term approaches zero. So, this term does not lead to any numerical difficulties.

Two series of calculations have been made to illustrate the properties of the SK model for small fields.

The object of the first series of calculations is to show how the shape and composition of the dips in the photoresponse depend on the recombination lifetime and the strength of the acoustic phonon

coupling. For this purpose, we consider recombination lifetimes of the order of the optical phonon lifetime at points 1 meV above the phonon emission threshold $\tau_r = 10^{-12}$ sec and an order of magnitude smaller, $\tau_r = 10^{-11}$ sec. The decomposition of the dips as a function of injection energy is displayed by a solid line representing the total photocurrent and a broken line representing the current, Eqs. (25) and (29), from electrons which have been scattered conservatively, if at all. Of course, the difference between the solid and broken lines is the photocurrent carried by electrons which have been inelastically scattered by an optical phonon to a state with energy near the bottom of the conduction band. In all calculations, the electric field is taken to be 10 V/cm. The

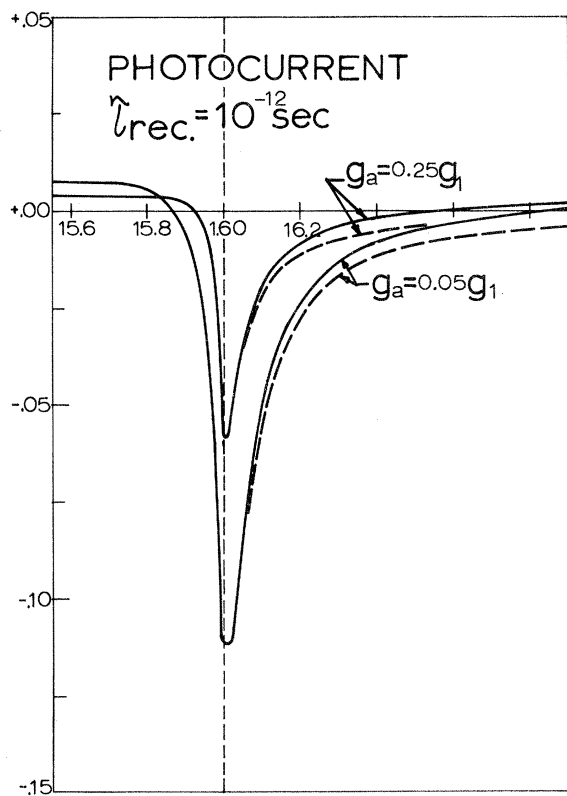


FIG. 2. The composition of dips in the photocurrent. The photoresponse current is plotted as a function of electron injection energy (meV) near an optical phonon emission threshold at 16 meV. The recombination lifetime is 10^{-12} sec. The largest negative current occurs when the acoustic phonon coupling is weak $g_a = 0.05g_1$. Strengthening the acoustic phonon coupling to $g_a = 0.25g_1$ reduces the minimum photocurrent by a factor of 2. In each case, the solid line is the total current and the broken line is that part of the current from the asymmetric distribution of electrons with energies near the phonon emission threshold energy.

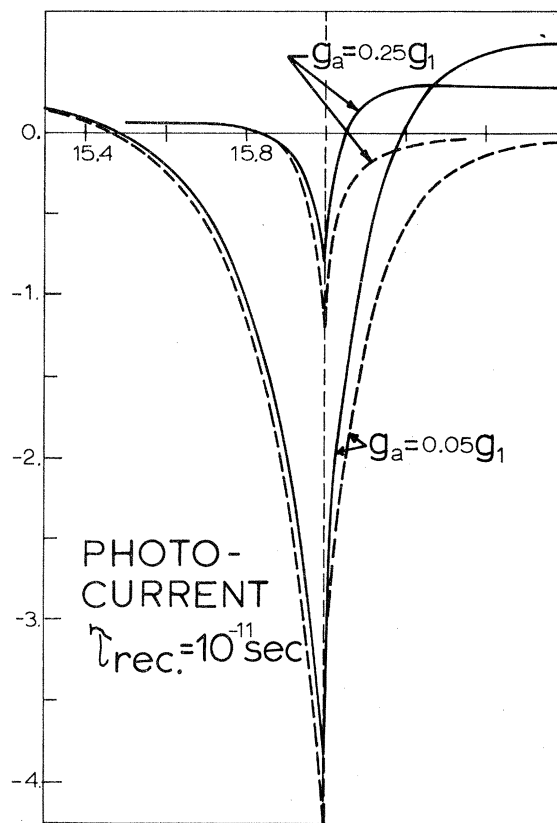


FIG. 3. The composition of dips in the photocurrent. The recombination lifetime 10^{-11} sec is increased by a factor of 10 and the other conditions of Fig. 2 are maintained. The effect of strengthening the acoustic phonon coupling is markedly different from that in Fig. 2.

small-field condition is satisfied because $F \times 10^{-11} \text{ sec} \sim 10^{-1} (\text{meV})^{1/2}$.

Normally, oscillatory photoconductivity is observed at low temperatures where acoustic phonon coupling is weak. In Fig. 2 are shown the effects of strengthening the acoustic phonon coupling from $g_a = 0.05g_1$ to $g_a = 0.25g_1$ in the case that the recombination lifetime is 10^{-12} sec. The same calculations repeated, but with the recombination lifetime increased to 10^{-11} sec, are shown in Fig. 3. It is evident that the effect of strengthening the acoustic phonon coupling becomes more pronounced when the recombination lifetime is increased. As the acoustic scattering becomes comparable to the inelastic scattering near the phonon-emission threshold, the existence of the threshold becomes less important. Eventually, as the temperature is increased the dip will be completely obliterated by the acoustic phonons.

The origin of negative current becomes apparent upon examination of the results shown in Figs.

2 and 3. Electrons injected into the conduction band near a phonon emission threshold will be evenly divided into those which have a component of momentum in the direction of the electric field and those which do not. The energy of those having a momentum component in the field direction will be increased by the action of the field, thereby increasing the probability that they will be scattered inelastically. The energy of those with a momentum component antiparallel to the field is first decreased by the field, hence decreasing the probability of inelastic scattering, before it is increased. The net effect is an asymmetry in the electron momentum distribution in opposition to the field. Of course, the inelastically scattered electrons may carry current if they are not lost by some recombination process. As the injection energy increases past the phonon emission threshold, the negative photoresponse current decreases and is more than balanced by the current carried by the inelastically scattered electrons. Thus, there is a dip in the photoresponse. The possibility that the total photocurrent will be negative is controlled mainly by the recombination lifetime. The recombination lifetime must be sufficiently short that more electrons are in the asymmetric momentum distribution near the phonon emission threshold than are accumulated nearer the bottom of the conduction band. Of course, these remarks do not consider such practical problems as actually realizing monoenergetic electron injection.

The second series of calculations considers the effect of competition between distinct optical phonons. For this purpose, we set the acoustic phonon coupling constant $g_a = 0.05g_1$ and the recombination lifetime $\tau_r = 10^{-11}$ sec. Using the small-field model defined above with the parameters just given, the dip at 16 meV will be repeated with very little change at 32 and 48 meV. However, this periodic appearance of the dips may not persist if there is another phonon mechanism operative. Suppose that an optical phonon mechanism with an emission threshold at 25 meV is turned on. The emergence of structure at 25 meV and how this affects the dip at 32 meV is shown in Fig. 4. Each curve is labeled with the relative value g_2/g_1 of the 25-meV optical phonon coupling constant. It is clear that the periodic repetition of dips in the photoresponse can be affected and even terminated by a sufficiently strong competing optical phonon mechanism. Such an effect, apparently, has been observed by Onton⁴ in the extrinsic photoconductivity of Si.

At first glance, the absence of a dip near the 25-meV optical phonon emission threshold may be unexpected. Indeed, if the current contributions were dissected as in the first series of calculations,

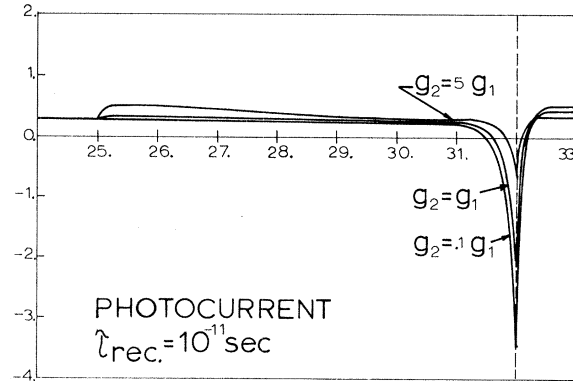


FIG. 4. Competition between optical phonon emission processes. A phonon of energy 25 meV is introduced. As the coupling parameter g_2 is increased from $0.1g_1$ to $5g_1$, some structure appears for injection near 25 meV and the dip near 32 meV is diminished. Each curve is labeled by the parameter g_2 . The acoustic phonon coupling parameter is $g_a = 0.05g_1$.

the current from the electrons with energies near the injection energies would show a small negative dip near the phonon emission threshold. However, for injection below the 25-meV threshold most of the electrons are scattered by emission of 16-meV phonons and the current is dominated by these scattered electrons with energies near 9 meV. As the injection energy is increased past the 25-meV threshold, the total current actually rises as a significant number of electrons are scattered inelastically to the bottom of the conduction band where the mobility is highest. The dip near 32-meV electron injection energy is dominated by electrons which have been scattered inelastically by 16-meV phonons and is diminished by the action of the 25-meV phonons.

V. DISCUSSION AND CONCLUSIONS

After introducing the SK model, we have presented an exact steady-state solution of the SK Boltzmann equation. For general fields and coupling parameters, it may be difficult to evaluate the exact solution. However, for small fields we have shown that it is possible to define a model of photoconductivity based on the exact solution which retains in a physically realizable context the essential features giving structure in the photoresponse. Furthermore, the small-field model of photoconductivity is eminently suitable for calculation.

The phenomenon of oscillatory photoconductivity as understood here permits very limited phonon spectroscopy. The exact solution and the small-field model provide the possibility of interpreting

and correlating information on the coupling parameters and recombination processes on a quantitative basis. Hence, the details of the structure observed in photoconductivity may serve a useful purpose and not be just a novelty.

The properties of the small-field model of photoconductivity have been exhibited by calculations appropriate to a nonpolar semiconductor. The calculations display graphically the origin of the dips in the photoresponse and indicate conditions which must be satisfied if such oddities as a current moving in opposition to the field are to be observed. It also is clear that a finite field is an essential requirement for the observation of dips. The field must be able to move an electron across a phonon emission threshold in an electron lifetime. The oscillatory structure is lost in the small-field limit. Although no calculations were presented specifically to illustrate field dependence, it is evident that the width of the dips is directly related to the fields. It is also evident from the calculations that the "intensity" of the dips in gen-

eral has no simple relation to the electron-phonon coupling constant.

In no case has the model led to predictions contrary to the general experimental trends.² Thus, detailed calculations for comparison with experiment are in order. It is evident that some of the restrictions that have been imposed on the small-field model may be relaxed and the region of validity of the model extended. However, it seems most fruitful to do this within the context of a specific physical system. Such calculations are in progress for the case of the extrinsic photoconductivity of silicon.

ACKNOWLEDGMENTS

A portion of the research reported here was performed while the author was a participant in the Faculty Research Program of Argonne National Laboratory. In this regard, it is a pleasure to acknowledge the hospitality of the Argonne Solid State Science Division and stimulating discussions with members of the solid-state theoretical group.

*Work supported in part by the Office of Naval Research under Themis Contract No. N00014-68-A-0504 and the Faculty Research Participation Program of Argonne National Laboratory.

¹R. F. Blunt, *Bull. Am. Phys. Soc.* **3**, 115 (1968).

²A survey of experimental observations of oscillatory photoconductivity is given in Table I, p. 614, of the

paper by H. J. Stocker, H. Levinstein, and C. R. Standard, Jr., *Phys. Rev.* **150**, 613 (1966).

³A. Onton, *Phys. Rev. Letters* **22**, 288 (1969).

⁴H. J. Stocker and H. Kaplan, *Phys. Rev.* **150**, 619 (1966).

⁵C. Herring and E. Vogt, *Phys. Rev.* **101**, 944 (1956).

⁶N. O. Folland, *Phys. Rev. B* **1**, 1648 (1970).